Electronic Supplementary Material (ESI) for ChemComm.
This journal is © The Royal Society of Chemistry 2019

Composite of high percentage exposed (00*l*) facets single-crystalline Bi_2WO_6 and polycrystalline BiOCl for highly efficient photocatalytic degradation of organic pollutants

Qing Yang, Maolan Luo, Kewei Liu, Hongmei Cao, Hongjian Yan*

College of Chemistry, Sichuan University, Chengdu, Sichuan, 610065, China
E-mail: hjyan@scu.edu.cn;
Tel: +86-1355-1341-892

Experimental Section

Materials

$Bi(NO_3)_3 \cdot 5H_2O$, $Na_2WO_4 \cdot 2H_2O$, polytetrafluoroethylene (PTFE), nitric acid, NaCl, and KCl were purchased from Kelong Chemistry Reagent Co. Ltd. (Chengdu, China). All the chemicals were used as received without any further purification.

Fabrication of BWO-PMS

Firstly, 10 mmol $Bi(NO_3)_3 \cdot 5H_2O$ and 5 mmol Na_2WO_4 were dissolved in 5 mL nitric acid (1:1) and 20 mL deionized water, respectively. After being mixed these two solutions and adjusted the pH to 5~6 by using ammonia, white precipitant produced. After being stirred for 10 min, the white precipitant was collected by filtration, followed by washing with deionized water and drying at 80 ^{o}C. Secondly, after being mixed with NaCl, KCl and PTFE, the precipitant was sintered under different conditions. Finally, after being cooled down to room temperature, the sintered mixture was washed with deionized water several times to remove salts and dried at 80 ^{o}C over night. For comparison, other samples were also prepared as the same procedure but without PTFE or using other additives, such as NaF, NH_4F, polyethylene (PE), or polyvinyl chloride (PVC).

Photocatalytic activity measurement

The photocatalytic activity of sample was investigated by degradation of RhB under visible light illumination (Ceralux 300W Xe lamp equipped with filter of $\lambda >$ 420 nm). Typically, 100 mg photocatalyst powder was added into 100 mL RhB solution (10 mg/L). After being stirred for 30 min in dark to achieve adsorption-desorption equilibrium, the solution was irradiated by visible light. The change of concentration of RhB was monitored by UV-Vis absorption curves collected on a Mapada UV-Vis spectrophotometer.

Characterization

XPS and energy-dispersive spectroscopy (EDS) data were collected on X-ray photoelectron spectroscopy (XPS, XSAM 800) and scanning electron microscopy (SEM, JSM-5900LV), respectively. The phase of samples were measured by powder X-ray diffraction (XRD) (EMPYREAN) at 40kV and 30mA with Cu-Kα radiation in the region of 5~70°. The morphology was characterized via scanning electron microscopy (SEM, JSM-5900LV) and transmission electron microscopy (TEM, Tecnai G2 F20 S-TWIN). UV-vis diffuse reflectance spectra were collected with a Shimadzu UV3600 spectrophotometer in the scan region of 200-800nm. The photoluminescence (PL) measurements were conducted on Hitachi F-7000 fluorescence spectrophotometer at the excitation wavelength of 280 nm. DMPO spin-trapping ESR spectra was obtained via Bruker EPR A300 and the sample was prepared by dispersing the powder in the methanol solution. Photoelectric chemical test was conducted on CHI660E electrochemical workstation with Pt counter electrode, Ag/AgCl reference electrode and working electrode. The preparation of the working electrode was as follow: 80 μL isopropyl alcohol, 250 μL deionized water, 10μL nafion solution, and 4mg sample were mixed and ultrasonic treated for 30 minutes. Subsequently, 40 μL of the mixture was used to smear 1cm^2 film on conductive glass, dried at 80 °C over night.

Figures and Tables

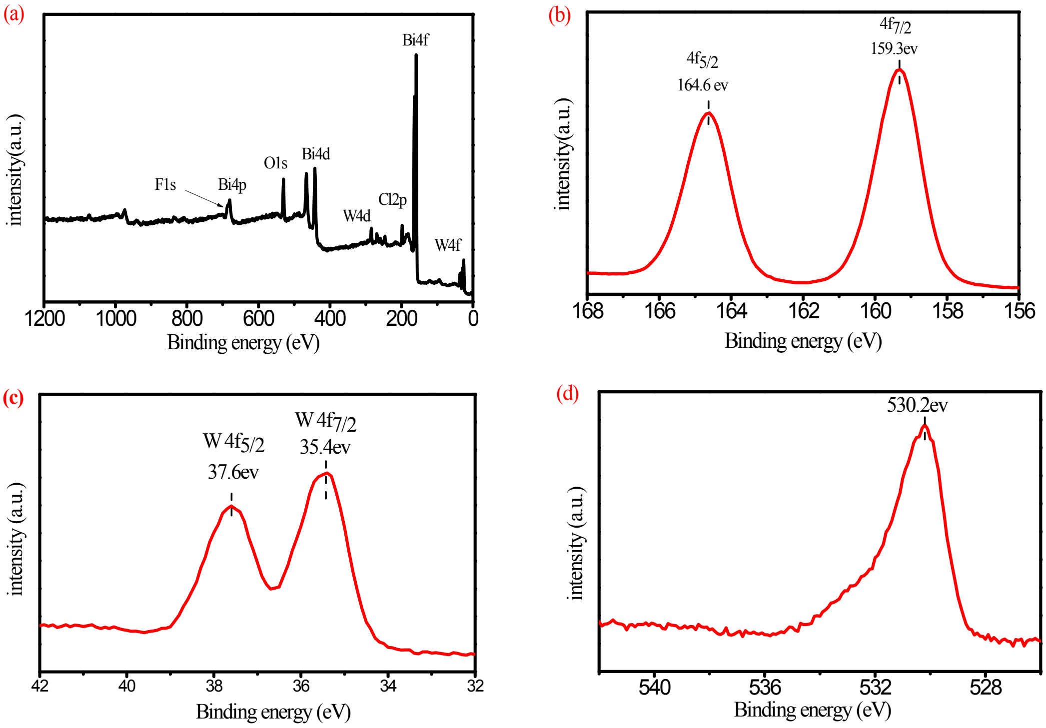

Figure S1. The XPS spectra of BWO-PMS. (a) survey scan, (b) Bi 4f, (c) W 4f, (d) O1s.

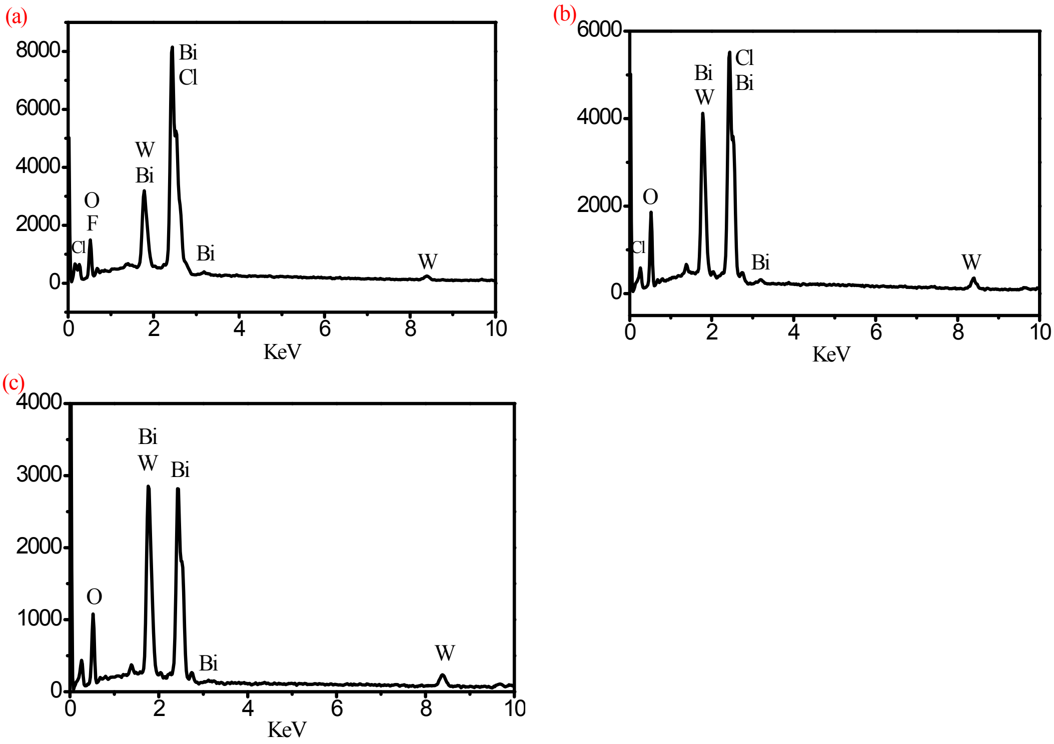

Figure S2. EDS spectra of BWO-PMS (a), BWO-MS (b), and BWO (c).

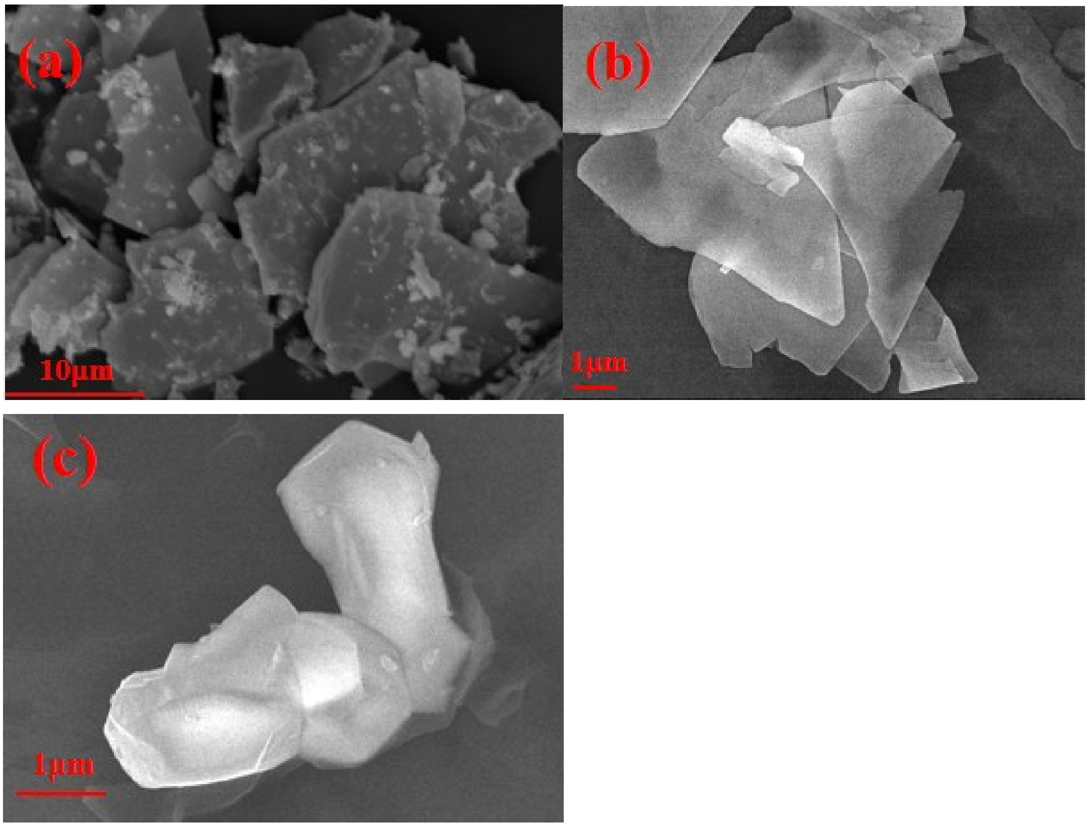

Figure S3. SEM image of BWO-PMS (a), BWO-MS (b), and BWO (c).

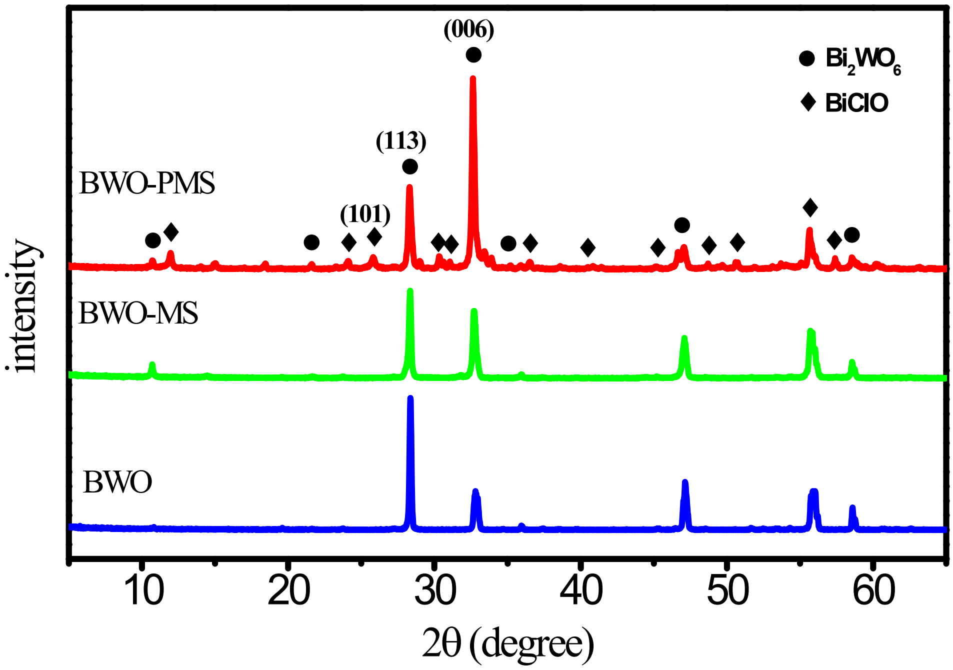

Figure S4. XRD patterns of BWO-PMS, BWO-MS, and BWO.

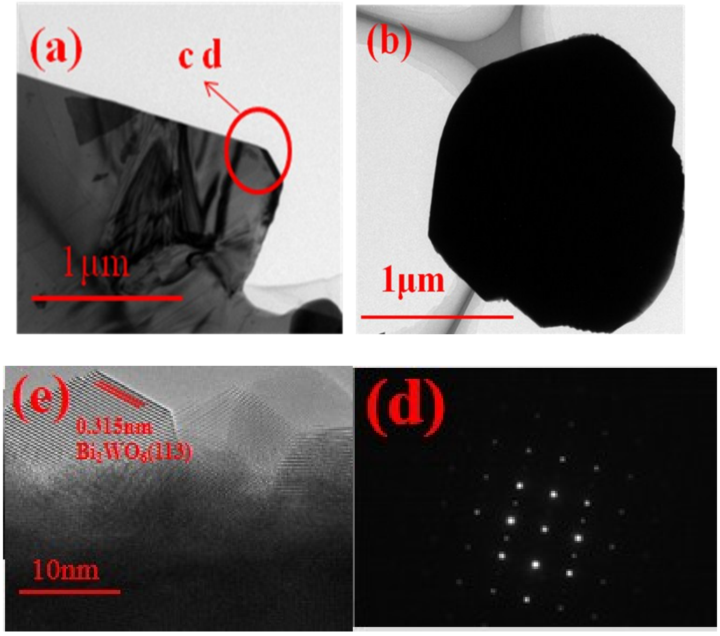

Figure S5. TEM image of BWO-MS (a), and BWO (b). (c) and (d) shows HRTEM image and SAED patterns of BWO-MS.

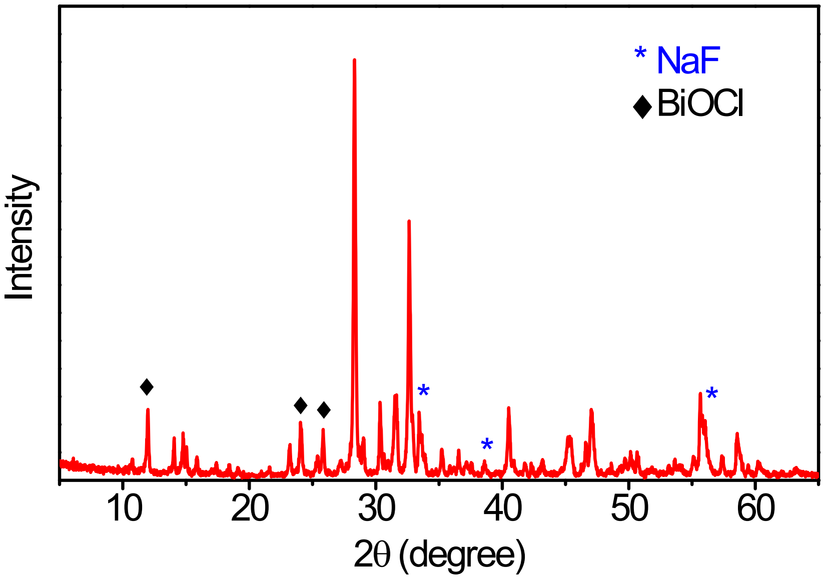

Figure S6. XRD patterns of unwashed BWO-PMS.

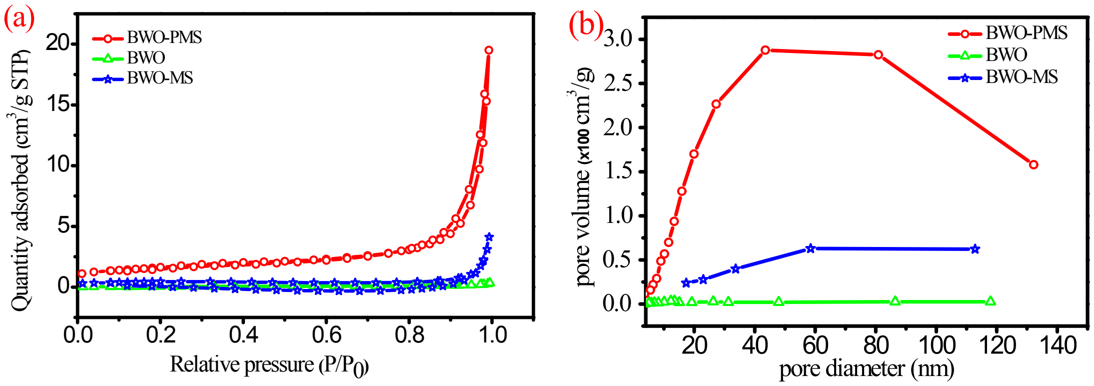

Figure S7. Nitrogen adsorption-desorption isotherm (a) and pore size distribution (b) of samples.

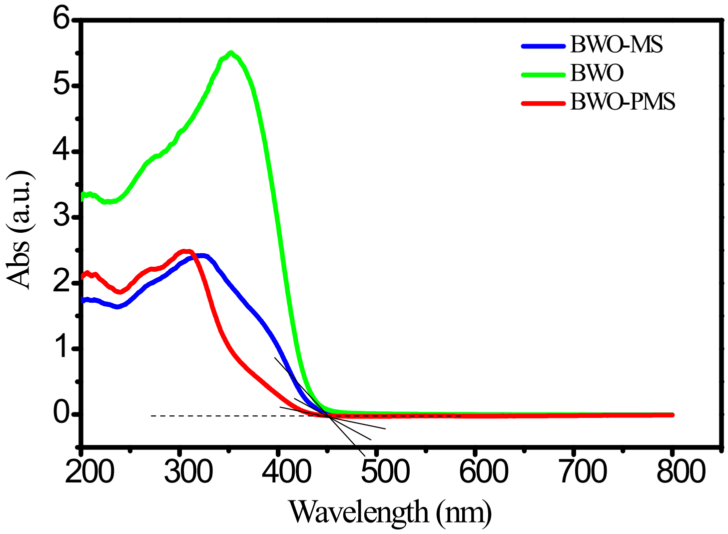

Figure S8. UV-vis diffuse reflectance spectra of BWO, BWO-MS, and BWO-PMS

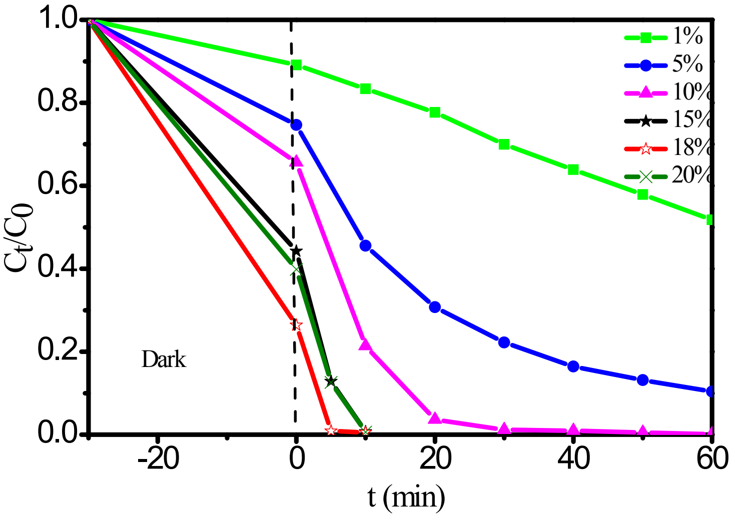

Figure S9. The photodegradation efficiency of BWO-PMS prepared with different amount of PTFE

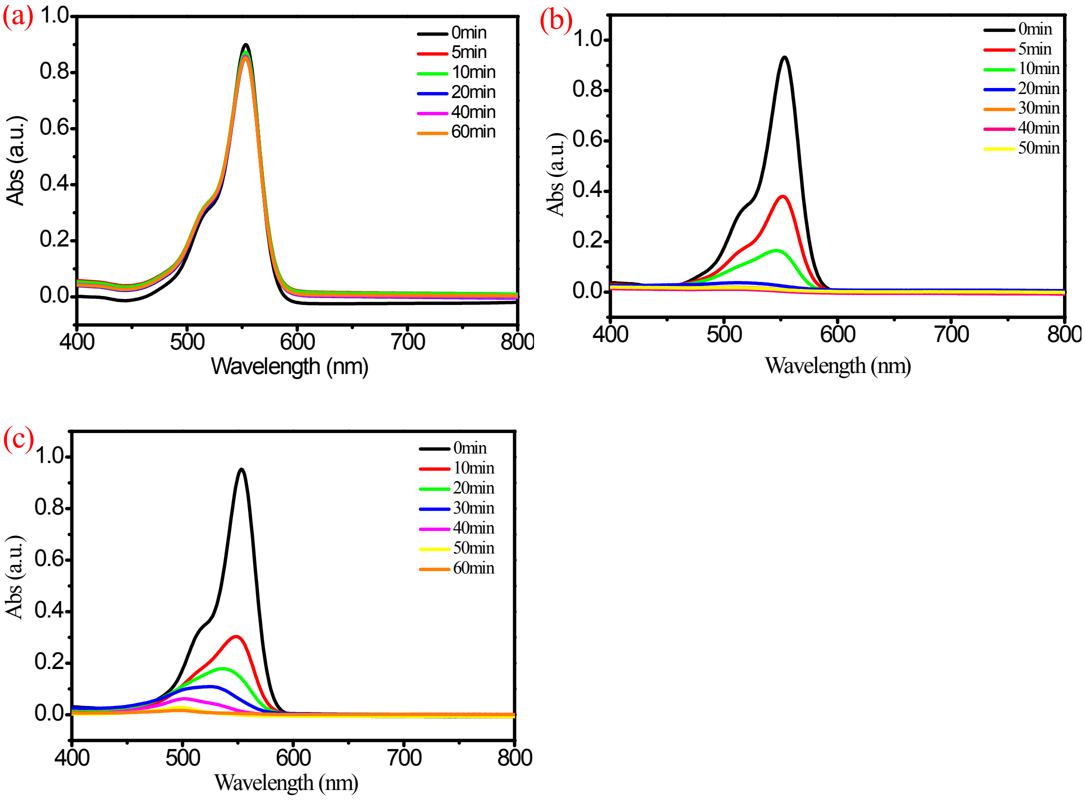

Figure S10. UV-vis spectra of RhB at different irradiation times degraded by Bi_2WO_6 prepared using NaF (a), NH_4F (b), as additives, and Bi_2WO_6 prepared via hydrothermal method (c).

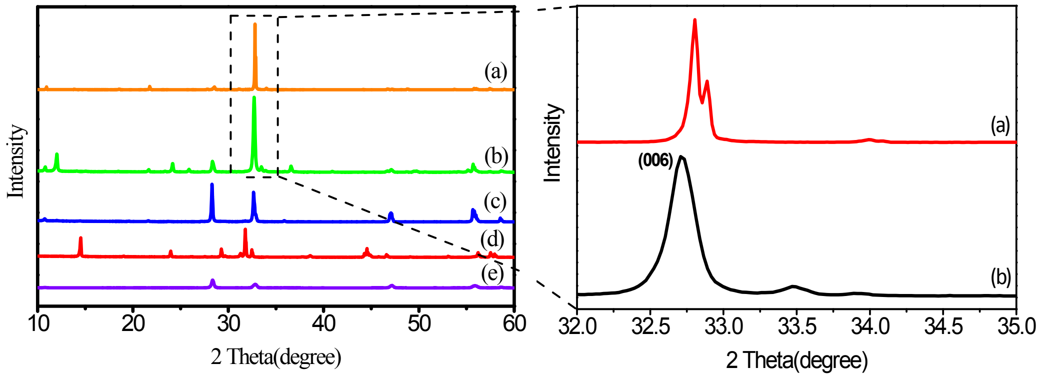

Figure S11. XRD patterns of samples prepared by MSM. (Left) Samples (a-d) were prepared by using NaCl-KCl as molten salt and PE (a), NH_4F (b), PVC (c), NaF (d) as additives, respectively. Sample (e) was prepared by using $NaNO_3/KNO_3$ as molten salt. (Right) The enlarged XRD patterns of (a) and (b) in the range of 32° ~35° .

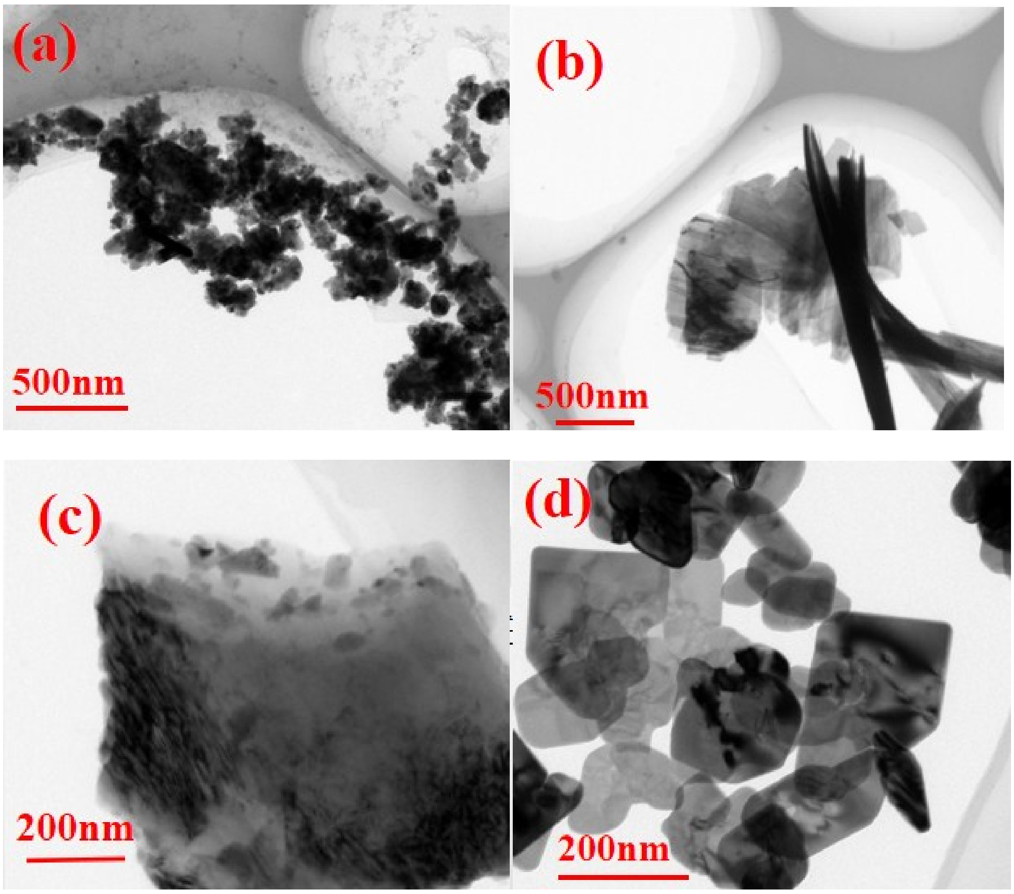

Figure S12. The TEM image of samples prepared by using NaCl-KCl as molten salt and NH_4F (a), PE (b), and NaF (c) as additive, respectively. (d) The TEM image of sample prepared by using $NaNO_3$/KNO_3 as molten salt.

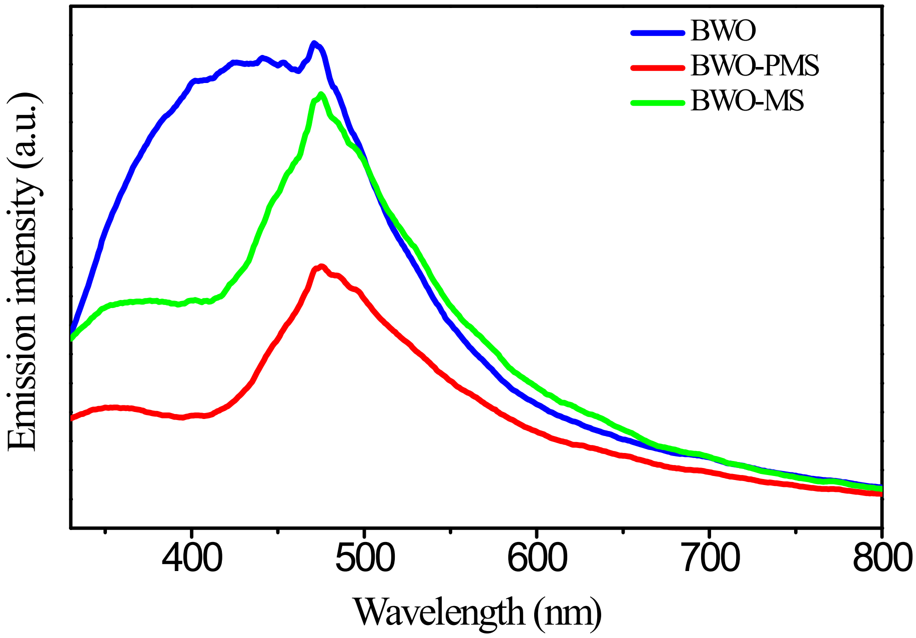

Figure S13. PL spectra of BWO, BWO-PMS, and BWO-MS.

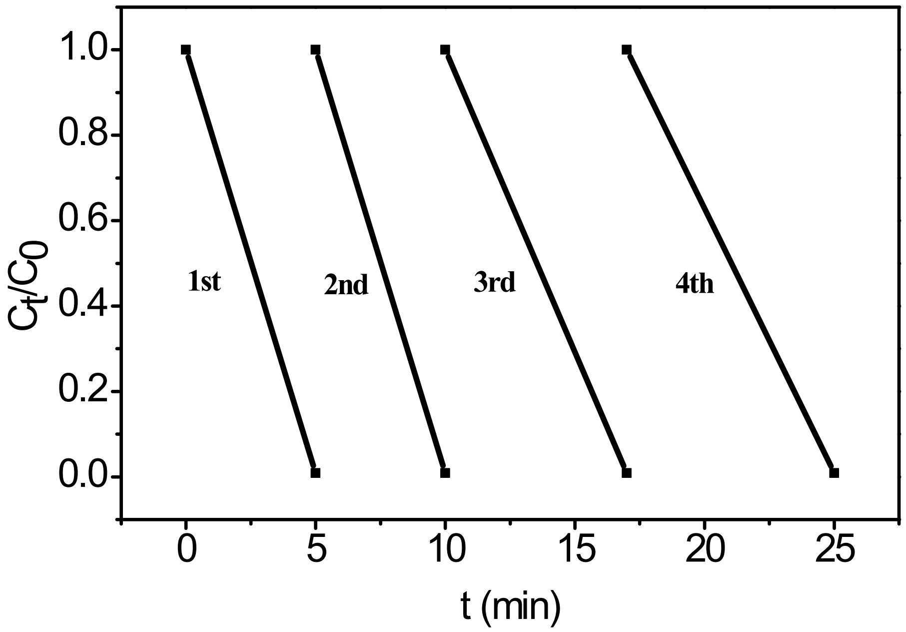

Figure S14. The cycle test results for photocatalytic degradation of RhB over BWO-PMS.

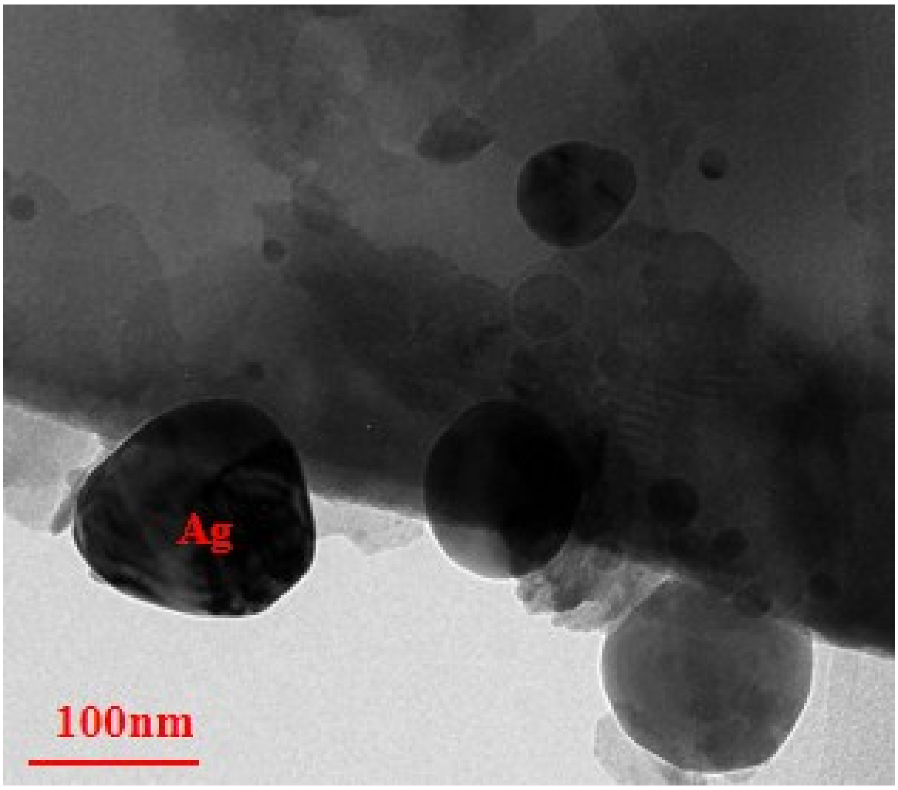

Figure S15. The TEM image of BWO-PMS after illumination in the presence of $AgNO_3$.

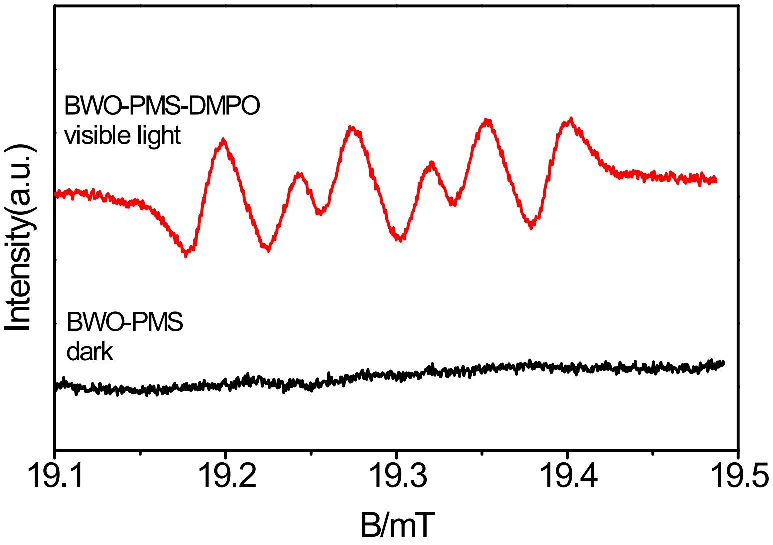

Figure S16. DMPO spin-trapping ESR spectra of BWO-PMS in methanol dispersion for DMPO-$\cdot O_2^-$.

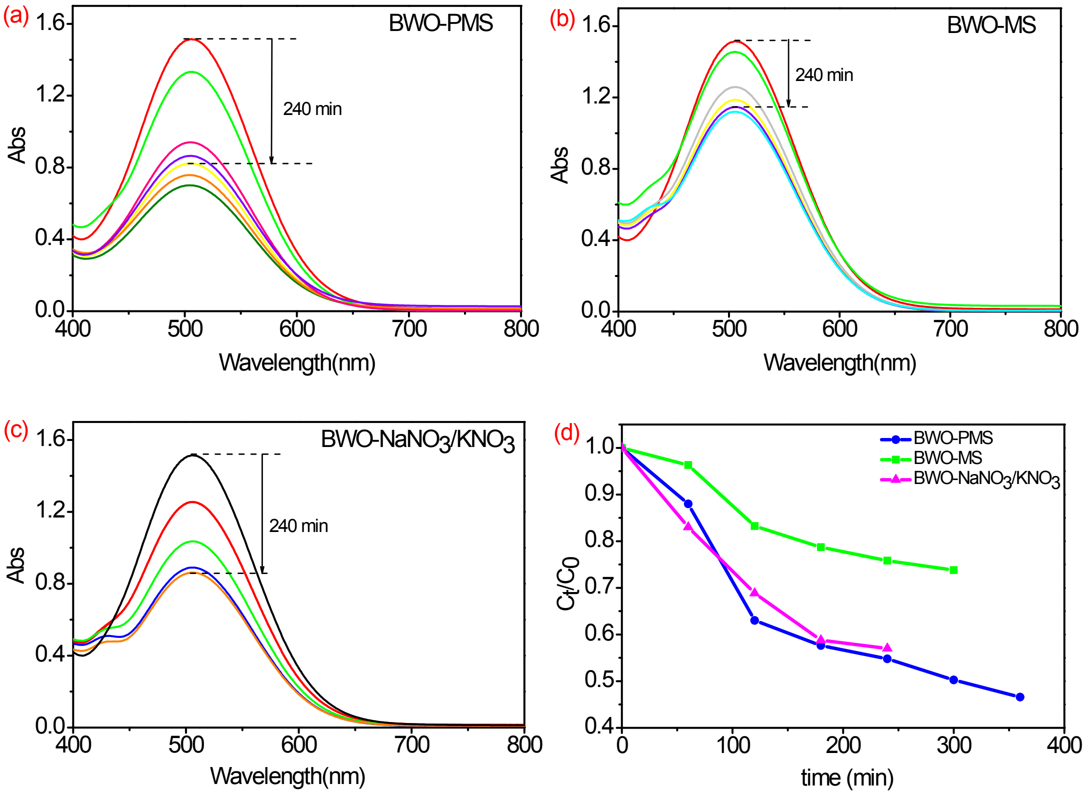

Figure S17. UV-vis spectra of phenol degraded by BWO-PMS (a), BWO-MS (b), and sample prepared by $NaNO_3/KNO_3$ molten salt (c). (d) shows the photodegradation efficiency of phenol over different photocatalysts under visible light illumination.

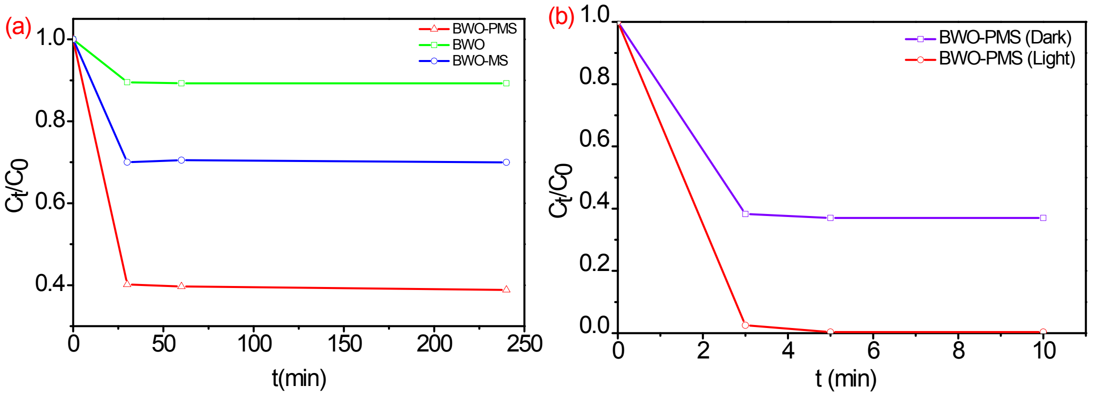

Figure S18. (a) The change of RhB concentration over different samples without illumination. (b) The change of RhB concentration over BWO-PMS with and without illumination, respectively.

Table S1. BET surface area of samples

Sample	BWO	BWO-MS	BWO-PMS	BWO-NH_4F
BET surface area(m^2/g)	0.23	1.52	5.85	2.47